Dinuclear Zinc Complexes Based on Parallel β-Diiminato Binding Sites: Syntheses, Structures, and Properties as CO_2/Epoxide Copolymerization Catalysts

Maurice Frederic Pilz,[†] Christian Limberg,*[,†] Boyan B. Lazarov,[‡] Kai C. Hultzsch,*[,‡] and Burkhard Ziemer[†]

Institut für Chemie, Humboldt-Universität zu Berlin, Brook-Taylor-Strasse 2, 12489 Berlin, Germany, and Institut für Organische Chemie, Friedrich-Alexander Universität Erlangen-Nürnberg, Henkestrasse 42, 91054 Erlangen, Germany

Received March 8, 2007

With the background that β-diketiminato zinc complexes efficiently catalyze the CO_2/epoxide copolymerization via a mechanism involving two catalyst molecules, a ligand system containing two parallel β-diiminato binding sites linked by a xanthene backbone ($[^{R}Xanthdim]^{2-}$ with residues R = 2,3-dimethylphenyl and 2,4-difluorophenyl at the iminato units, respectively) was investigated with respect to its zinc coordination chemistry. The corresponding diimines $[^{R}Xanthdim]H_2$ were treated with diethylzinc to yield the complexes $[^{Me2C6H3}Xanthdim](ZnEt)_2$, **4**, and $[^{F2C6H3}Xanthdim](ZnEt(thf))_2$, **5**, respectively. In order to convert these compounds into polymerization catalysts, they were subsequently treated with SO_2, which indeed resulted in the corresponding ethylsulfinates. Due to aggregation via intermolecular bridging of ethylsulfinate ligands, the product after the reaction of **5** represents an insoluble coordination polymer. Aggregation does take place also for the primary product obtained from the reaction of **4**, as evidenced by the isolation of the tetramer $[\{[^{Me2C6H3}Xanthdim]Zn_2(\mu\text{-}O_2SEt)\}\mu\text{-}O_2SEt]_4$, **6**, and the precipitation of an insoluble solid on storing of such mixtures. **4**, **5**, and **6** display moderate activities as catalysts for the copolymerization of cyclohexene oxide and CO_2. A bimodal molecular weight distribution points to two effective mechanisms, one of which probably involves two cooperating Zn centers as anticipated. Possible structural reasons for these catalytic results are discussed.

Introduction

CO_2 is an inexpensive, nontoxic, totally renewable feedstock, whose reduction would have a positive impact on the global carbon balance, and these facts alone are sufficient motivation for producing chemicals from CO_2 whenever possible.[1] After early work in the area of polymers, recent years gave rise to a number of new homogeneous catalysts for the copolymerization of CO_2 and oxiranes to form polycarbonates (eq 1).[2]

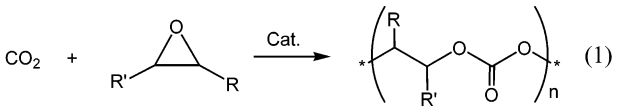

(1)

These discrete catalysts allow for more rapid and selective polymerizations in comparison to the heterogeneous matches; that is, research of the last years has increased the productivity of this reaction by ca. 100 times and also has expanded the range of applicable oxiranes. While a large number of catalysts are known today, only a few of them reach the activity of zinc complexes.[3] G. W. Coates and co-workers discovered a highly active, living polymerization system at low pressures and temperatures based on β-diketiminato-zinc catalysts. In order to prepare these, a mononuclear ethyl zinc precursor complex (Scheme 1a) is treated with alcohols or acetic acid to give dinuclear alkoxides and acetates, respectively.[2e,h,4] Activation of the ethyl precursors can also proceed via treatment with SO_2, which gives rise to ethylsulfinates.[5] Solution studies hinted at monomer/dimer equilibria dependent on the counteranions, and on the basis of stoichiometric insertion studies and kinetic investigations a mechanism was suggested involving two zinc diketiminate units (Scheme 1b).[3a] This and other examples where two diketiminato metal units cooperate in the activation of a certain substrate,[6] as well as the fact that bimetallic catalysis is also utilized by many metalloenzymes,[7] stimulated us to think

* Corresponding authors. Reprint requests to C.L. Fax: +49 30 2093 6966. E-mail: Christian.limberg@chemie.hu-berlin.de.
[†] Humboldt-Universität zu Berlin.
[‡] Friedrich-Alexander Universität Erlangen-Nürnberg.

(1) Arakawa, H.; Aresta, M.; Armor, J. N.; Barteau, M. A.; Beckman, E. J.; Bell, A. T.; Bercaw, J. E.; Creutz, C.; Dinjus, E.; Dixon, D. A.; Domen, K.; Dubois, D. L.; Eckert, J.; Fujita, E.; Gibson, D. H.; Goddard, W. A.; Goodman, D. W.; Keller, J.; Kubas, G. J.; Kung, H. H.; Lyons, J. E.; Manzer, L. E.; Marks, T. J.; Morokuma, K.; Nicholas, K. N.; Periana, R.; Que, L.; Rostrup-Nielson, J.; Sachtler, W. M. H.; Schmidt, L. D.; Sen, A.; Somorjai, G. A.; Stair, P. C.; Stults, B. R.; Tumas, W. *Chem. Rev.* **2001**, *101*, 953.

(2) (a) Darensbourg, D. J.; Holtcamp, M. W. *Macromolecules* **1995**, *28*, 7577. (b) Darensbourg, D. J.; Holtcamp, M. W. *Coord. Chem. Rev.* **1996**, *153*, 155. (c) Super, M. S.; Berluche, E.; Costello, C. A.; Beckman, E. J. *Polym. Mat. Sci. Eng. Prepr.* **1996**, *74*, 430. (d) Super, M. S.; Beckman, E. J. *Macromol. Symp.* **1998**, *127*, 89. (e) Cheng, M.; Lobkovsky, E. B.; Coates, G. W. *J. Am. Chem. Soc.* **1998**, *120*, 11018. (f) Beckman, E. *Science* **1999**, *283*, 946. (g) Nazaki, K.; Nakano, K.; Hiyama, T. *J. Am. Chem. Soc.* **1999**, *121*, 1108. (h) Cheng, M.; Darling, N. A.; Lobkovsky, E. B.; Coates, G. W. *J. Chem. Soc., Chem. Commun.* **2000**, 2007.

(3) (a) Review on Zn-based catalysts: Coates, G. W.; Moore, D. R. *Angew. Chem., Int. Ed.* **2004**, *43*, 6618. (b) Cr-Salen complexes with high activity: Darensbourg, D. J.; Mackiewicz, R. M.; Phelps, A. L.; Billodeaux, D. R. *Acc. Chem. Res.* **2004**, *37*, 836. Darensbourg, D. J.; Mackiewicz, R. M.; Rodgers, J. L.; Phelps, A. L. *Inorg. Chem.* **2004**, *43*, 1831. Darensbourg, D. J.; Mackiewicz, R. M.; Billodeaux, D. R. *Organometallics* **2005**, *24*, 144.

(4) (a) Cheng, M.; Moore, D. R.; Reczek, J. J.; Chamberlain, B. M.; Lobkovsky, E. B.; Coates, G. W. *J. Am. Chem. Soc.* **2001**, *123*, 8738. (b) Moore, D. R.; Cheng, M.; Lobkovsky, E. B.; Coates, G. W. *Angew. Chem.* **2002**, *114*, 2711; *Angew. Chem., Int. Ed.* **2002**, *41*, 2599. (c) Allen, S. D.; Moore, D. R.; Lobkovsky, E. B.; Coates, G. W. *J. Am. Chem. Soc.* **2002**, *124*, 14284.

(5) Eberhardt, R.; Allmendinger, M.; Luinstra, G. A.; Rieger, B. *Organometallics* **2003**, *22*, 211.

10.1021/om070221e CCC: $37.00
Publication on Web 06/14/2007

Scheme 1. (a) β-Diketiminato Ethyl Zinc Precursor, (b) Suggested Transition State of the Epoxide Ring Opening (R = Polymer)

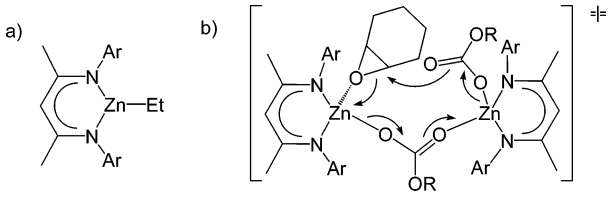

about the design of a ligand containing two diiminato moieties in close proximity. Some ligands fulfilling this requirement have already been described; in most of these examples the diiminato moieties are incorporated into a macrocyclic ring system,[8] in other cases two N atoms belonging to different diiminato units are linked,[9] and in all these compounds the chelating functions are arranged face to face. Inspired by the above-mentioned work by Coates et al., some of them, for instance *o*-phenylene-bridged bis(anilido-aldimine) compounds, were employed to synthesize dinuclear zinc complexes, which indeed proved to be significantly more active than mononuclear versions, at least under very diluted conditions.[8c]

We were interested in synthesizing a ligand where the two diiminato units are oriented parallel to each other, to investigate the difference this makes for the cooperative behavior of the two metal centers.

Hence, recently we reported the synthesis of $[^{Me2C6H3}Xanthdim]H_2$ (Scheme 2), where this idea is realized.[10] Here we describe the derivatization of $[^{R}Xanthdim]H_2$, the syntheses of corresponding zinc complexes, and the results of tests concerning their catalytic activity in the epoxide/CO_2 copolymerization.

Results and Discussion

Ligand Synthesis. The synthesis of $[^{Me2C6H3}Xanthdim]H_2$ reported[10] starts from the diol **2**, which can be prepared from the dibromide **1** (Scheme 2). **2** then has to be converted into the dicarboxylic acid **3** via initial OH/Br and Br/CN exchange followed by acidic hydrolysis. A Vilsmeier type of reaction then leads to a double vinamidinium salt, which is hydrolyzed, and the last step in the reaction sequence consists of an anilation reaction through which the residues R are introduced. So far only one derivative containing 2,3-dimethylphenyl substituents,

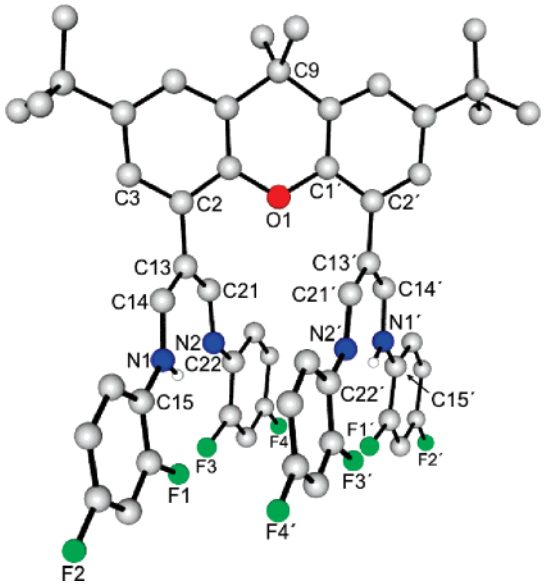

Figure 1. Structure of one of the two independent molecules of $[^{F2C6H3}Xanthdim]H_2$ found in the elemental cell of its crystals. A cocrystallized molecule of chloroform and hydrogen atoms [apart from the ones at N(1) and N(1′)] are omitted for clarity.

Table 1. Selected Bond Lengths [Å] and Angles [deg] for $[^{F2C6H3}Xanthdim]H_2$

N(1)−H(1)	0.88(4)	N(2)−H[N(1)]	1.987(4)
C(15)−N(1)	1.405(5)	C(14)−N(1)	1.343(5)
C(14)−C(13)	1.373(5)	C(13)−C(21)	1.436(5)
C(21)−N(2)	1.294(5)	C(22)−N(2)	1.410(5)
C(14)−N(1)−H(1)	116.4(4)	C(13)−C(14)−N(1)	124.0(4)
C(14)−C(13)−C(21)	122.8(3)	C(13)−C(21)−N(2)	122.0(4)
C(21)−N(2)−C(22)	121.2(4)		
C(3)−C(2)−C(13)−C(14)	46.8(5)	C(1′)−C(2′)−C(13′)−C(21′)	50.6(5)
C(13)−C(14)−N(1)−C(15)	2.7(4)	C(13)−C(21)−N(2)−C(22)	2.5(3)
N(1)−C(15)−C(16)−F(1)	3.5(6)	N(2)−C(22)−C(23)−F(3)	3.5(10)

$[^{Me2C6H3}Xanthdim]H_2$, has been described. Here we report a second one, $[^{F2C6H3}Xanthdim]H_2$ (see Scheme 2), that can be obtained analogously and might be an alternative, if electron-withdrawing residues are required. Figure 1 shows the molecular structure of $[^{F2C6H3}Xanthdim]H_2$ adopted in the crystal (one of two independent molecules present in the unit cell), and Table 1 lists its relevant bond lengths and angles. The crystallographical C_2-axis goes right through the center of the molecule (C(9)−

Scheme 2

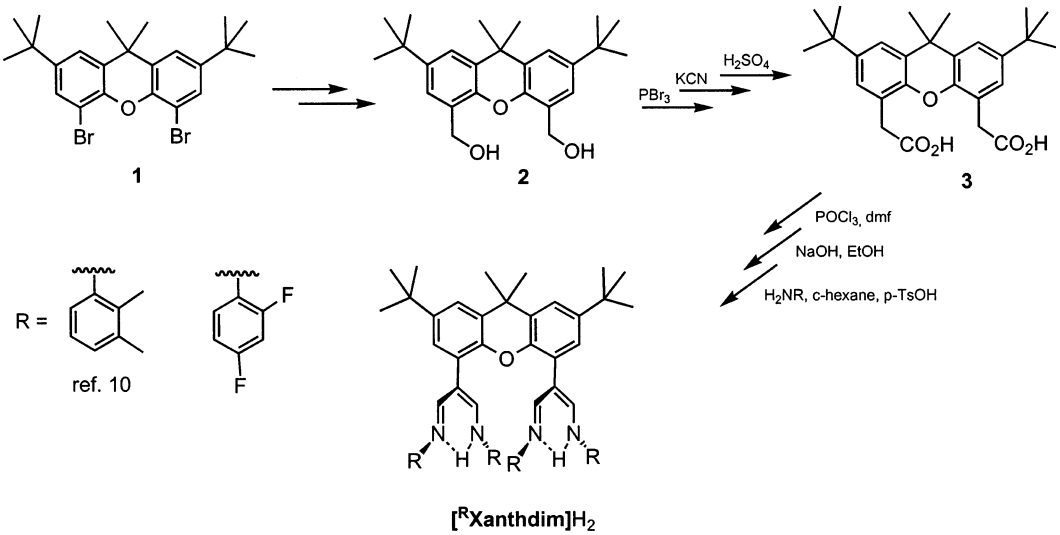

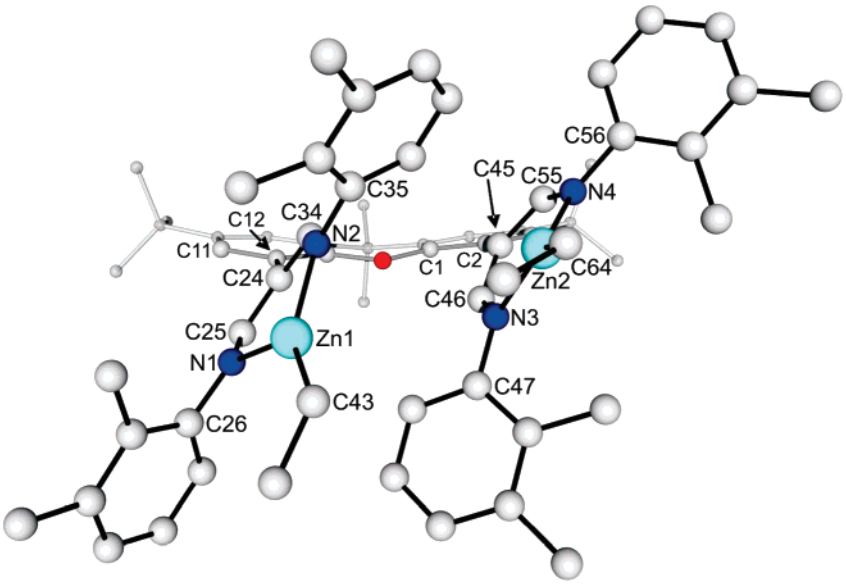

Figure 2. Molecular structure of **4**. Hydrogen atoms are omitted for clarity.

Scheme 3

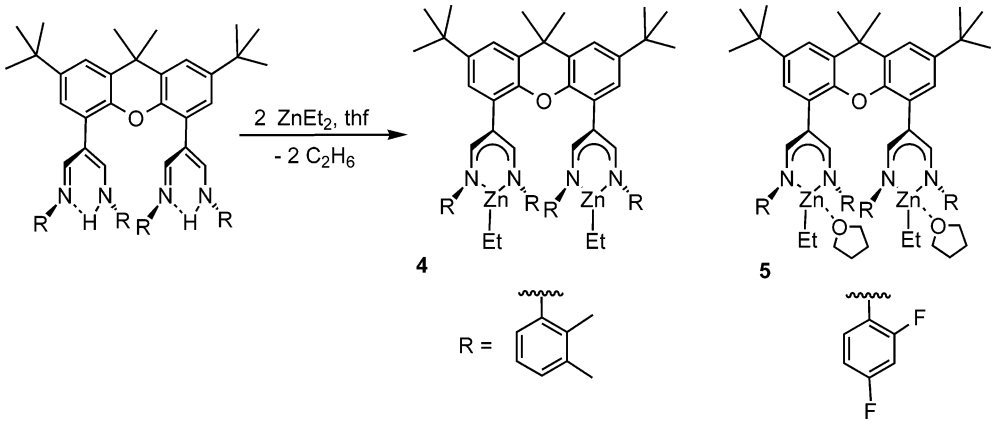

O(1)). As in the molecular structure of [^{Me2C6H3}Xanthdim]H_2,[10] the C═N and C═C bonds are localized within the β-diimine units, and this also becomes evident in the solution NMR spectra of [^{F2C6H3}Xanthdim]H_2. Within each of the diimine moieties the distance between the fluorine atom in *ortho*-position of one of the 2,4-difluorophenyl rings and the amine proton H(N) is less than the sum of van der Waals radii, giving rise to hydrogen bonding (F1−H[N(1)]: 2.276(3) Å). This and the sterically undemanding nature of the fluorine atoms (in comparison to the methyl groups in [^{Me2C6H3}Xanthdim]H_2) are the reason for the almost perfectly coplanar β-diimine units. The distance between them amounts to ca. 4.5 Å.

Complex Synthesis and Structures. In order to prepare dinuclear Zn complexes of the potential ligands [^{Me2C6H3}Xanthdim]$^{2-}$ and [^{F2C6H3}Xanthdim]$^{2-}$, the protonated forms were treated with 2 equiv of $ZnEt_2$. This led to the complexes [^{Me2C6H3}Xanthdim]-$(ZnEt)_2$, **4**, and [^{F2C6H3}Xanthdim]$(ZnEt(thf))_2$, **5** (Scheme 3), which can be isolated in pure form after removing all volatiles under vacuum and recrystallization. **4** and **5** were characterized by means of IR and NMR spectroscopy as well as by elemental analysis. In addition, single crystals could be grown, and the results of the X-ray diffraction analyses are shown in Figures 2 and 3 (Tables 2 and 3 list relevant bond lengths and angles).

In **4** each Zn atom has a trigonal planar coordination environment consisting of the two N atoms of the β-diiminato ligand and the terminal ethyl ligand (sum of angles around the Zn atoms: Zn(1): 360.1° and Zn(2): 359.5°). These planes are somewhat tilted with respect to the planes defined by the diiminato units in a way that brings the two Zn atoms closer together. The Zn−Zn separation of 4.922 Å is significantly shorter than that reported for a dinuclear zinc complex,[8b] 6.010 Å, containing one of the above-mentioned macrocyclic bis-β-diiminato ligands. As the two Zn diiminato units are not oriented perfectly parallel to each other and as additionally the xanthene backbone is somewhat distorted in the crystal structure—probably due to packing effects—the Zn−Zn distance can be expected to be even shorter in a relaxed structure in solution. Within each of the individual units the Zn−N bond distances are equivalent [Zn(1)−N(1): 1.995 Å, Zn(1)−N(2): 1.997 Å, Zn(2)−N(3): 2.002 Å, and Zn(2)−N(4): 2.000 Å], and the same is true for the corresponding C−N and C−C bonds, which points to an efficient delocalization of the π-electrons. As in the case of the lithium salt of [^{Me2C6H3}Xanthdim]$^{2-}$, the diiminato moieties are twisted[10] with respect to the xanthene backbone (C(1)−C(2)−C(45)−C(55): 44.1° and C(11)−C(12)−C(24)−C(34): 62.7°).

The structure of **5** is similar to that of **4**, but each Zn ion coordinates a thf molecule in addition, thereby reaching a—in Zn chemistry rarely observed[8b,11]—distorted trigonal pyramidal coordination sphere, where the thf ligand occupies the axial position [sum of angles for the Zn−N and Zn−C bonds around the zinc ions: Zn(1), 353.5°; Zn(2), 348.3°]. In **5** the two Zn

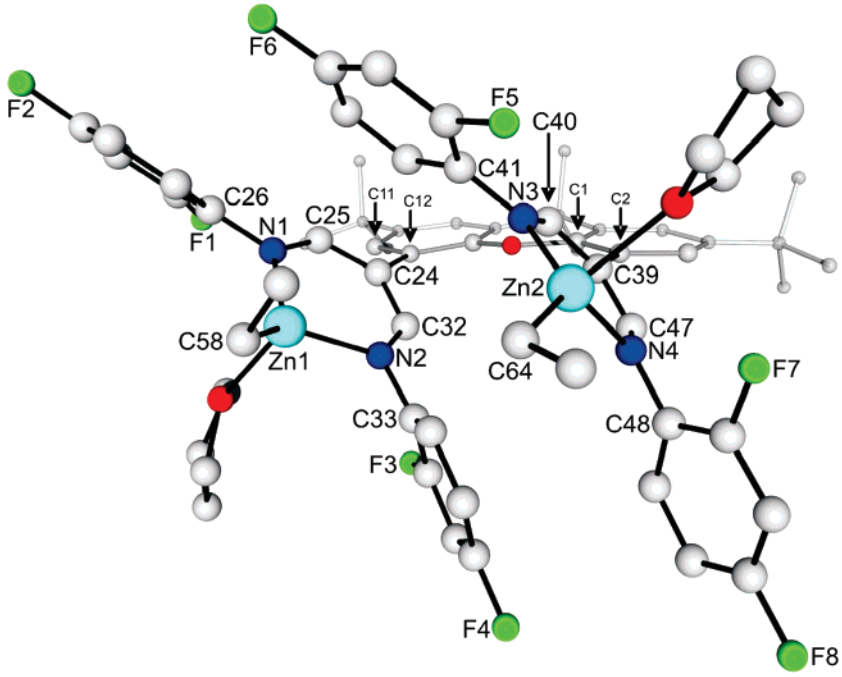

Figure 3. Molecular structure of **5**. Hydrogen atoms and two cocrystallized molecules of thf are omitted for clarity.

Table 2. Selected Bond Lengths [Å] and Angles [deg] for Compound 4

Zn(1)−Zn(2)	4.922(1)		
Zn(1)−N(1)	1.995(2)	Zn(1)−N(2)	1.997(2)
Zn(2)−N(3)	2.002(2)	Zn(2)−N(4)	2.000(2)
Zn(1)−C(43)	1.978(3)	Zn(2)−C(64)	1.963(3)
N(1)−C(26)	1.425(1)	N(1)−C(25)	1.325(3)
C(25)−C(24)	1.398(4)	C(24)−C(34)	1.402(4)
C(34)−N(2)	1.334(3)	N(2)−C(35)	1.428(3)
C(47)−N(3)	1.429(4)	N(3)−C(46)	1.333(3)
C(46)−C(45)	1.391(4)	C(45)−C(55)	1.396(4)
C(55)−N(4)	1.331(3)	N(4)−C(56)	1.434(4)
N(1)−Zn(1)−N(2)	92.75(9)	N(1)−Zn(1)−C(43)	128.0(2)
C(26)−N(1)−C(25)	117.7(2)	N(1)−C(25)−C(24)	127.1(2)
C(25)−C(24)−C(34)	124.0(2)	C(24)−C(34)−N(2)	126.7(3)
C(34)−N(2)−C(35)	116.9(2)	N(3)−Zn(2)−N(4)	93.63(9)
N(3)−Zn(2)−C(64)	134.0(2)	C(47)−N(3)−C(46)	115.7(2)
N(3)−C(46)−C(45)	127.4(2)	C(46)−C(45)−C(55)	124.2(2)
C(45)−C(55)−N(4)	127.9(3)	C(55)−N(4)−C(56)	115.8(2)
C(24)−C(25)−N(1)−Zn(1)	13.3(4)	C(45)−C(46)−N(3)−Zn(2)	10.4(4)
C(11)−C(12)−C(24)−C(34)	62.7(3)	C(1)−C(2)−C(45)−C(55)	44.1(3)

Table 3. Selected Bond Lengths [Å] and Angles [deg] for 5

Zn(1)−Zn(2)	5.6038(8)		
Zn(1)−N(1)	2.005(2)	Zn(1)−N(2)	2.017(3)
Zn(2)−N(3)	2.033(2)	Zn(2)−N(4)	2.032(2)
Zn(1)−C(58)	1.973(3)	Zn(2)−C(64)	1.972(3)
C(26)−N(1)	1.421(4)	N(1)−C(25)	1.326(4)
C(25)−C(24)	1.400(4)	C(24)−C(32)	1.407(4)
C(32)−N(2)	1.322(4)	N(2)−C(33)	1.421(4)
C(41)−N(3)	1.420(4)	N(3)−C(40)	1.336(4)
C(40)−C(39)	1.395(4)	C(39)−C(47)	1.400(4)
C(47)−N(4)	1.329(3)	N(4)−C(48)	1.422(4)
N(1)−Zn(1)−N(2)	93.69(9)	N(1)−Zn(1)−C(58)	131.8(2)
C(26)−N(1)−C(25)	118.7(2)	N(1)−C(25)−C(24)	127.7(2)
C(25)−C(24)−C(32)	125.6(3)	C(24)−C(32)−N(2)	125.6(3)
C(32)−N(2)−C(33)	118.2(3)	N(3)−Zn(2)−N(4)	93.17(9)
N(3)−Zn(2)−C(64)	131.4(2)	C(41)N(3)−C(40)	115.0(2)
N(3)−C(40)−C(39)	127.1(2)	C(40)−C(39)−C(47)	126.0(2)
C(39)−C(47)−N(4)	126.6(3)	C(47)−N(4)−C(48)	116.2(2)
C(11)−C(12)−C(24)−C(25)	43.7(4)	C(1)−C(2)−C(39)−C(40)	51.1(5)

ions are positioned almost exactly within the planes defined by the diiminato units (C(24)−C(25)−N(1)−Zn(1): 2.4(4)°, C(39)−C(40)−N(3)−Zn(2): 6.9(4)°), and the high symmetry within the diiminato units again points to an effective delocalization of the π-electron density. Only a slight folding can be observed for the xanthene backbone, but the Zn diiminato units are directed away from each other so that the Zn−Zn distance is larger than in **4** (5.6038 Å). The Zn−N and Zn−C bond lengths of both compounds **4** and **5** are comparable to those previously described for zinc atoms coordinated by β-diketiminato and alkyl ligands.[4a,c,5,12]

As outlined in the Introduction, for catalytic applications zinc alkyl complexes are not ideally suited as precursors, so that they are usually converted to the corresponding acetates, alkoxides, or alkylsulfinates for this purpose. We decided to follow the alkylsulfinato approach and therefore reacted **4** and **5** dissolved in toluene or thf with SO_2. In the case of **4** this leads to a yellow solution, and after removal of all volatiles a yellow solid is obtained that can be redissolved readily in thf. Storing this solution at rt leads to the precipitation of a yellow solid that analyzes as $[^{Me2C6H3}Xanthdim](Zn(O_2SEt))_2$ and cannot be brought back into solution.

Addition of hexane to the above-mentioned thf solution leads to yellow crystals, which were investigated also by means of

(6) (a) Dai, X.; Warren, T. H. *J. Am. Chem. Soc.* **2004**, *126*, 10085. (b) Smith, J. M.; Lachicotte, R. L.; Holland, P. L. *Chem. Commun.* **2001**, 1542. (c) Smith, J. M.; Lachicotte, R. L.; Pittard, K. A.; Cundari, T. R.; Lukat-Rodgers, G.; Rodgers, K. R.; Holland, P. L. *J. Am. Chem. Soc.* **2001**, *123*, 9222.

(7) McCleverty, J. A., Meyer, T. J., Eds. (Que, L., Jr., Tolman, W. B., Vol. Eds.) *Comprehensive Coordination Chemistry II*; Elsevier: Oxford 2004, Vol. 8, Chapters 8.1, 8.10, 8.13, 8.15, 8.19, 8.24.

(8) (a) Curtis, N. F. In *Comprehensive Coordination Chemistry II*; McCleverty, J. A., Meyer, T. J., Eds. (Lever, A. B. P., Vol. Ed.); Elsevier: Oxford, 2004; Vol. 1, Chapter 1.20. (b) Lee, S. Y.; Na, S. J.; Kwon, H. Y.; Lee, B. Y.; Kang, S. O. *Organometallics* **2004**, *23*, 5382. (c) Lee, B. Y.; Na, S. J.; Kwon, H. Y.; Lee, S. Y.; Na, S. J.; Han, S.; Yun, H.; Lee, H. Park, Y.-W. *J. Am. Chem. Soc.* **2005**, *127*, 3031.

(9) (a) Bourget-Merle, L.; Hitchcock, P. B.; Lappert, M. F. *J. Organomet. Chem.* **2004**, *689*, 4357. (b) Vitanova, D. V.; Hampel, F.; Hultzsch, K. C. *J. Organomet. Chem.* **2005**, *690*, 5182. Also compare: Allen, S. D.; Moore, D. R.; Lobkovsky, E. B.; Coates, G. W. *J. Organomet. Chem.* **2003**, *683*, 137, for an alternative approach, involving, however, oxo imido units.

(10) Pilz, M. F.; Limberg, C.; Ziemer, B. *J. Org. Chem.* **2006**, *71*, 4559.

(11) Sun, X. X.; Qi, C.-M.; Ma, S.-L.; Huang, H.-B.; Zhu, W.-x.; Liu, Y.-C. *Inorg. Chem. Commun.* **2006**, *9*, 911.

(12) (a) Moore, D. R.; Cheng, M.; Lobkovsky, E. B.; Coates, G. W. *J. Am. Chem. Soc.* **2003**, *125*, 11911. (b) Chisholm, M. H.; Gallucci, J.; Phomphrai, K. *Inorg. Chem.* **2002**, *41*, 2785.

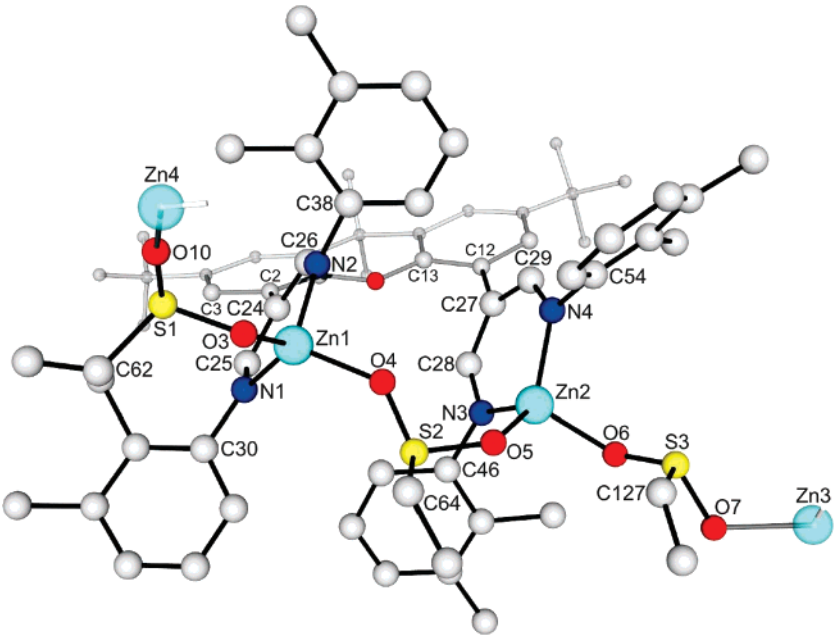

Figure 4. One monomeric unit of the tetrameric structure found for **6** (compare Figure 5). Hydrogen atoms are omitted for clarity.

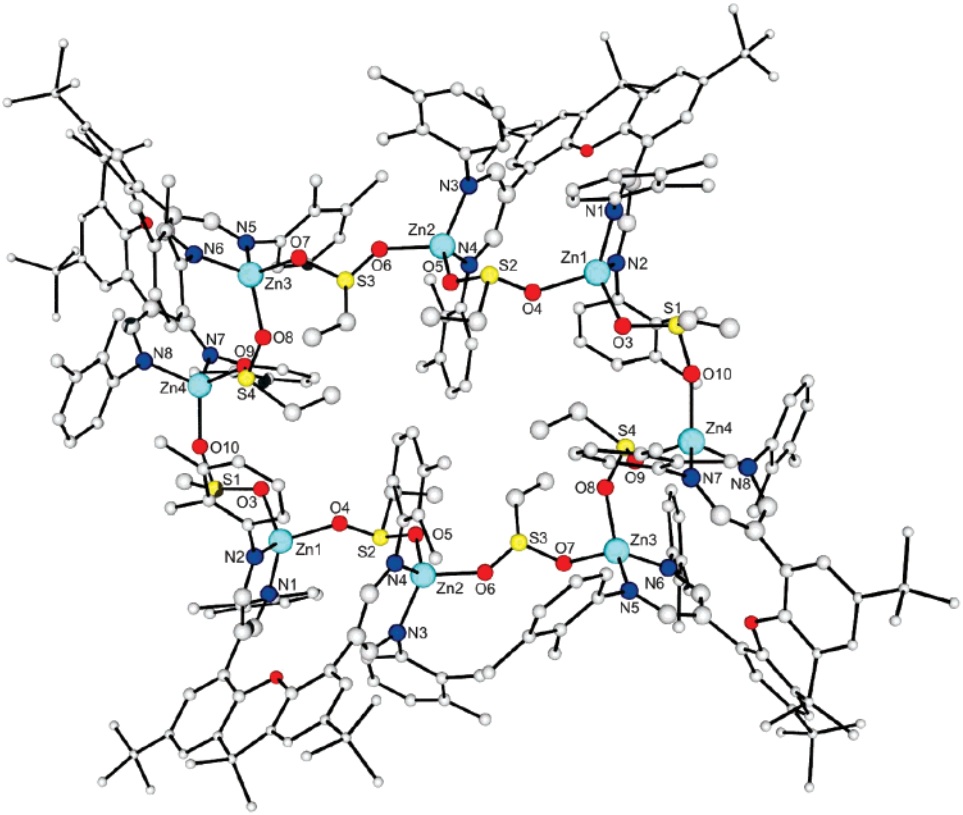

Figure 5. View of the 32-membered ring of the tetramer **6**. Hydrogen atoms are omitted for clarity.

X-ray diffraction. The result is shown in Figures 4 and 5 as well as in Scheme 4. As intended, SO_2 has inserted into all Zn−C bonds so that ethylsulfinate anions were formed, one of which is found in a bridging position between the two Zn ions coordinated to a certain Xanthdim ligand (Figure 4). Within these anions the S−O bond lengths are quite similar [S(2)−O(4): 1.48(2) Å, S(2)−O(5): 1.53 (2) Å, S(4)−O(8): 1.498(9) Å, S(4)−O(9): 1.49(2) Å], and the same is true for the Zn−O bonds generated by their coordination, so that altogether the intramolecularly bridging ethylsulfinate anions are bonded symmetrically with delocalized charge. So far the principal connectivities are identical to the ones observed for the products of reactions between mononuclear diketiminato zinc alkyl complexes and SO_2. However, while in the latter case the remaining alkylsulfinato anion forms a second bridge between the two Zn centers, so that a dinuclear complex with a Zn-$(RSO_2)_2$Zn entity is stabilized,[3,5] the special design of the Xanthdim ligand system seems to make *inter*molecular interactions more favorable. In principle these could have led to a coordination polymer, but a ring structure is formed here (see Figure 5) involving four [^{Me2C6H3}Xanthdim](Zn(O_2SEt))$_2$ units that are linked via ethylsulfinato moieties to give the tetramer

Scheme 4

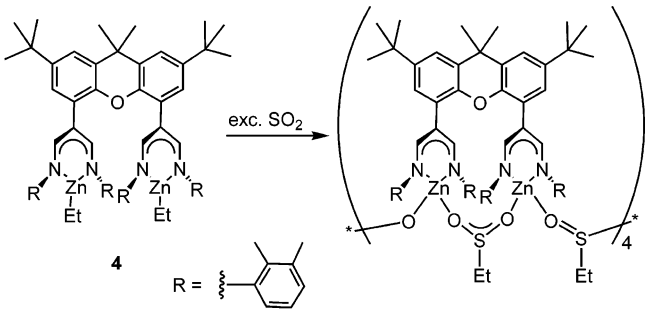

Table 4. Selected Bond Lengths [Å] and Angles [deg] for 6[a]

Zn(1)−Zn(2)	5.093(3)	Zn(1)−O(3)	1.933(8)
Zn(1)−O(4)	1.95(2)	Zn(1)−N(1)	1.953(9)
Zn(1)−N(2)	1.95(2)	Zn(2)−O(6)	1.89(2)
Zn(2)−O(5)	1.951(9)	Zn(2)−N(3)	1.950(9)
Zn(4)−N(4)	1.95(2)	S(2)−O(4)	1.48(2)
S(2)−O(5)	1.54(2)	S(2)−C(64)	1.79(2)
S(1)−O(3)	1.58(2)	S(1)−O(10)	1.46(2)
S(1)−C(62)	1.71(3)	S(3)−O(6)	1.39(2)
ul;1S(3)−O(7)	1.561(9)	S(3)−C(127)	1.71(2)
C(30)−N(1)	1.43(2)	N(1)−C(25)	1.33(2)
C(25)−C(24)	1.39(2)	C(24)−C(26)	1.40(2)
C(26)−N(2)	1.31(2)	N(2)−C(38)	1.47(2)
C(46)−N(3)	1.46(2)	N(3)−C(28)	1.30(2)
C(28)−C(27)	1.40(3)	C(27)−C(29)	1.40(3)
C(29)−N(4)	1.42(2)	N(4)−C(54)	1.43(2)
S(1)−O(10)	1.46(2)	Zn(3)−O(7)	1.934(9)
Zn(3)−O(8)	1.942(8)	S(4)−O(8)	1.498(9)
S(4)−O(9)	1.49(2)	Zn(4)−O(9)	1.98(2)
Zn(4)−O(10)	1.936(8)		
S(1)−O(3)−Zn(1)	117.6(6)	O(3)−Zn(1)−O(4)	99.2(5)
Zn(1)−O(4)−S(2)	131.1(8)	O(4)−S(2)−O(5)	107.6(7)
S(2)−O(5)−Zn(2)	125.3(5)	O(5)−Zn(2)−O(6)	98.6(5)
Zn(2)−O(6)−S(3)	140.4(7)	O(4)−S(2)−C(64)	101.0(8)
N(1)−Zn(1)−N(2)	97.9(4)	N(3)−Zn(2)−N(4)	97.4(4)
O(3)−Zn(1)−N(1)	116.5(4)	O(3)−Zn(1)−N(2)	117.5(5)
O(5)−Zn(2)−N(3)	114.6(4)	O(5)−Zn(2)−N(4)	120.0(4)
C(24)−C(25)−N(1)−Zn(1)	2(2)	C(27)−C(28)−N(3)−Zn(2)	7(2)
C(3)−C(2)−C(24)−C(26)	55(2)	C(13)−C(12)−C(27)−C(29)	47(2)

[a] Underlined bonds are part of the 32-membered ring.

[{[^{Me2C6H3}Xanthdim]Zn_2(μ-O_2SEt)}μ-O_2SEt]$_4$, **6**. As can be seen in Table 4, the intermolecularly bridging ethylsulfinato ligands are partially asymmetric, as indicated by two significantly different S−O and Zn−O bond distances within a certain Zn−O−S−O−Zn moiety (e.g., S(3)−O(6): 1.39(2) Å, S(3)−O(7): 1.561(9) Å) and partially symmetric (e.g., (S(1)−O(3): 1.58(2) Å, S(1)−O(10): 1.46(2) Å). Crystallographically the tetramer consists of a dimer of a dimer. The xanthene backbones are pointing outward and the N-bonded aryl rings are located above and below the 32-membered ring. The Zn−Zn distances within the individual [^{Me2C6H3}Xanthdim]Zn_2(μ-O_2SEt) units are quite similar (Zn(1)−Zn(2): 5.093(3) Å, Zn(3)−Zn(4): 5.182(3) Å) and much shorter than those found *between* such moieties (Zn(1)−Zn(4): 5.61(1) Å, Zn(2)−Zn(3): 5.96(1) Å). All Zn ions involved are coordinated tetrahedrally by the O atoms of two ethylsulfinate ligands and the two N atoms of a diiminato unit.

If an analogous reaction with SO_2 is performed starting from **5**, a yellow solid precipitates that cannot be redissolved or purified sufficiently to allow unequivocal identification. It can only be assumed that in the case of **5** a coordination polymer is formed that is insoluble and thus not employable as a homogeneous catalyst. According to LDI-ToF-MS measurements (see Figure 6), the product formed initially in the reaction between **4** and SO_2 is monomeric; no aggregated species could be detected in solution, but a degradation during the laser desorption cannot be excluded (in fact the broad signals observed in the NMR spectra and their behavior on variation of the temperature point to multiple dynamic processes and species in solution). Precipitation of an insoluble solid on aging of such solutions is probably caused by an aggregation process comparable to the one observed to occur spontaneously on treatment of **5** with SO_2. However, the rate of polymerization is much slower in the case of the primary product obtained from **4**, and **6** may be regarded as an intermediate (accordingly, storing of a solution of **6** also led to an insoluble solid).

Catalytic Activity. The bis(β-diiminatozinc) complexes **4**, **5**, and **6** were tested in the copolymerization of cyclohexene oxide (CHO) and CO_2 (Table 5). Complex **4** displayed moderate activity at 50 °C and 8 atm CO_2 in neat CHO, and the polymer product contained only 50% of carbonate linkages (Table 5, entry 1; compare for instance the results[4b] for one of the most active β-diketiminato zinc methoxide complexes under comparable conditions (entry 8): TOF = 2290 h^{-1}, 90% carbonate linkages, M_w/M_n = 1.09). Increasing the reaction temperature to 75 °C improved the content of carbonate linkages to 77% (Table 5, entry 2), but led to the formation of 3% cyclic carbonate byproduct and broadening of the molecular weight distribution. However, dilution of the reaction mixture with toluene (1:1 v/v) improved the carbonate linkage content to 91% and produced a polymer with a higher molecular weight and a narrower polydispersity of 1.7 (Table 5, entry 3 vs entry 2).

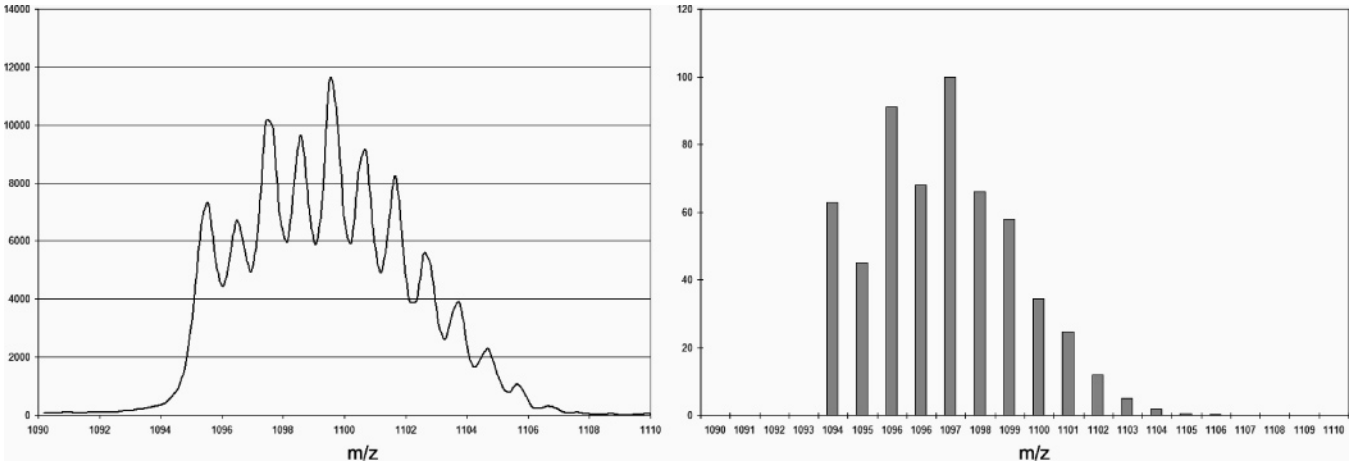

Figure 6. Measured M^+ peak in LDI-ToF-MS (left) and calculated spectra for [[^{Me2C6H3}Xanthdim]Zn_2(O_2SEt)]$^+$ (right).

Table 5. Copolymerization of Cyclohexene Oxide (CHO) and CO_2 Catalyzed by Bis-β-diiminato Zinc Complexes[a]

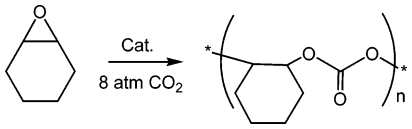

entry	cat.	T [°C]	t [h]	yield [mg]	TON	TOF [h^{-1}]	% carbonate linkages	% cyclic carbonate	M_n	M_w	M_w/M_n
1	**4**	50	72	1600	666	9.3	50	0.5	16 760	45 100	2.7
2	**4**	75	24	450	170	7.1	77	3	5970	23 300	3.9
3	**4**[b]	75	24	250	90	3.8	91	9	10 300	17 900	1.7
4	**5**	50	36	450	220	6.1	8	1	nd	nd	
5	**5**	75	72	800	380	5.3	15	1	nd	nd	
6	**6**	50	96	300	110	1.15	85	1	4840	15 800	3.3
7	**6**	75	48	750	285	5.9	76	2	4640	12 800	2.8
8[c]	**A**	50	0.17		382	2290	90		22 900	24 961	1.09
9[d]	**B**	60	3		651	217	96		49 600	64 480	1.3

[a] Reaction conditions: 40 mmol of CHO, 20 μmol of cat = 40 μmol of Zn ([CHO]:[Zn] = 1000:1); 8 atm of CO_2. [b] Reaction mixture was diluted with toluene (1:1 v/v). nd = not determined. [c] Ref 4b. [d] Ref 5. **A** = [{(2,6-$Me_2C_6H_3$)NC(Me)C(CN)C(Me)N(2,6-i-$Pr_2C_6H_3$)}Zn(OMe)]$_2$. **B** = [{(2,6-$Et_2C_6H_3$)NC(Me)CHC(Me)N(2,6-$Et_2C_6H_3$)}Zn(O_2SEt)]$_2$.

The fluorine-substituted complex **5** on the other hand produced a polymer containing predominantly ether linkages, presumably as a result of an increased Lewis acidity of the metal center due to the electron-withdrawing 2,4-difluorophenyl substituents, which supports the ring-opening polymerization of CHO. Most notably, the ethylsulfinate complex **6** displayed catalytic activity comparable to the ethyl zinc complex **4** only at 75 °C (Table 5, entry 7 vs entry 2), whereas a significantly lower activity, but higher carbonate linkage content was observed at 50 °C (Table 5, entry 6 vs entry 1, also compare entry 9, illustrating the results obtained for a highly active β-diketiminato zinc ethylsulfinate complex). The lower activity of **6** in comparison to **4** might result from the higher degree of aggregation within complex **6**, which might hamper the initiation of the polymerization. At higher temperature, a more rapid dissociation of the tetramer on the other hand should lead to more active species. In all cases the molecular weight distributions are bimodal, which could be interpreted in terms of two effective mechanisms, one of which probably involves two cooperating Zn centers as anticipated (the competing one might comprise individual, independent Zn centers without cooperation). However, probably the steric bulk within the reaction pocket overcompensates the positive effect of the cooperation supported by the dinucleating ligand system, so that the latter does not increase the efficiency.

Conclusions

A novel ligand system has been used to prepare dinuclear versions of previously known β-diketiminato zinc complexes that had proved efficient catalysts for the epoxide/CO_2 copolymerization. Two ligand versions were employed—one with electron-donating methyl substituents at the N-aryl donor functions and the other containing electron-withdrawing F atoms—to produce two complexes, each of which comprises two Zn-ethyl units. The latter can be readily converted into Zn-ethylsulfinato moieties via reaction with SO_2. Due to the bidentate character of the ethylsulfinato ligands, they give rise to aggregation reactions, which in the case of the more electron-deficient, fluorinated complex leads to an insoluble coordination polymer. In the case of the more electron-rich representative aggregation leads to a soluble tetramer with an interesting structural motif. This compound and the Zn-ethyl complexes were investigated as potential catalysts for the cyclohexene oxide/CO_2 copolymerization. While treatment with SO_2 was meant to activate the Zn-ethyl complexes for this type of reaction, interestingly the Zn-ethyl complexes proved to be more active than the Zn-O_2SEt tetramer (considering that mononuclear β-diketiminato Zn-ethyl complexes usually do not show any activity before activation; current research will therefore also deal with the CO_2 reactivity of **4** and **5**). A bimodal molecular weight distribution hints at a cooperation of the two Zn centers during the catalysis, as intended, but nevertheless the activity observed is only moderate. One explanation could be that the steric bulk within the reaction pocket overcompensates the positive effect the cooperation could have on the efficiency of the catalysis. Alternatively, the finding might indicate that the accessibility of a cooperative interaction as shown in Scheme 1b is a prerequisite for a high activity. Future studies will address this and other questions via further variation of the ligand system.

Experimental Section

General Procedures. Apart from the ligand synthesis, all manipulations were carried out in a glovebox or by means of Schlenk-type techniques involving the use of a dry argon atmosphere. The ^{1}H and ^{13}C NMR spectra were recorded on a Bruker AV 400 NMR spectrometer (^{1}H 400.13 MHz) or on a Bruker DPX 300 MHz (^{1}H 300.13 MHz, ^{13}C 75.5 MHz) with $CDCl_3$, C_6D_6, or thf-d_8 as solvent at 25 °C. The ^{1}H and ^{13}C NMR spectra were calibrated against the residual proton and natural abundance ^{13}C resonances of the deuterated solvent ($CDCl_3$ δ_H 7.24 ppm, δ_C 77.0 ppm; C_6D_6 δ_H 7.15 ppm δ_C 128.0 ppm; thf-d_8 δ_H 3.58 ppm, δ_C 67.7 ppm). Microanalyses were performed on a Leco CHNS-932 elemental analyzer. Infrared (IR) spectra were performed using samples prepared as KBr pellets on a Shimadzu FTIR-8400S spectrometer. LDI-ToF mass spectra were recorded with an Applied Biosystems Voyager-DE mass spectrometer without matrix using a laser wavelength of λ = 337 nm. The mass spectrum was calculated with the program Molecular Weight Calculator, Version 6.31, by Matthew Monroe. Solvents were dried using a Braun solvent purification system, degassed by a vacuum-freezing cycle, and stored above 4 Å molecular sieves. SO_2 gas was dried by passing it through a short column of P_4O_{10}, condensed in a Young-Schlenk tube at −30 °C that contained molecular sieve 4 Å, and stored for at least 24 h before use. Molecular weights of the polycarbonates were determined by GPC (Agilent 1100 Series using RI detector, 3 SDV linear M 5 μm columns with 8 × 50 mm, 8 × 300 mm, and 8 × 600 mm dimensions) versus polystyrene standards using THF at 35 °C as eluent.

2,7-Bis(1,1-dimethylethyl)-9,9-dimethyl-4,5-bis(1-(2,4-difluorophenylamino)-3-(2,4-difluorophenylimino)isopropenyl)xanthene, [^{F2C6H3}Xanthdim]H$_2$. The raw material (3.30 g, 6.74 mmol) obtained starting from **3** in the Vilsmeier-type reaction (Scheme 1) according to ref 10 was placed in a round-bottomed flask, dissolved in 150 mL of dry cyclohexane. Subsequently, 2,4-difluoroaniline (7.00 mL, 68.78 mmol) and *p*-toluenesulfonic acid (1.90 g, 9.98 mmol) were added, and the flask was connected to a Dean Stark apparatus with a drying tube on top. The mixture was heated under reflux for 5 days and then neutralized with a concentrated $NaHCO_3$ solution. The aqueous solution was extracted several times with a mixture of diethyl ether/tetrahydrofuran in a 2:1 ratio, and after drying the combined organic phases with magnesium sulfate all volatiles were removed from the filtrate under vacuum. To the resulting amber-colored oil was added 30 mL of absolute ethanol, and the mixture was heated to reflux. The yellow precipitate formed was recrystallized several times from absolute ethanol, and after sufficient drying *in vacuo* [^{F2C6H3}Xanthdim]H$_2$ was obtained (3.00 g, 3.31 mmol; solid; 43.8% yield with respect to **3** employed).

Table 6. Crystal Data for Compounds [^{F2C6H3}Xanthdim]H_2, 4, 5, and 6

	[^{F2C6H3}Xanthdim]H_2 (without solvent)	[^{F2C6H3}Xanthdim]H_2	**4**	**5**	**6**
formula	$C_{53}H_{46}F_8N_4O$	$C_{54}H_{47}Cl_3F_8N_4O$	$C_{65}H_{78}N_4OZn_2$	$C_{73}H_{86}F_8N_4O_5Zn_2$	$C_{67}H_{82}N_4O_{5.50}S_2Zn_2$
fw	906.94	1026.31	1062.05	1382.2	1226.23
space group	$P2_1/n$	*Pnna*	$P\bar{1}$	$P2_1/n$	$P\bar{1}$
a, Å	15.584(2)	16.073(5)	16.806(3)	15.955(2)	16.975(3)
b, Å	14.072(3)	16.716(5)	17.110(3)	18.698(3)	17.897(3)
c, Å	20.847(3)	18.411(7)	20.756(3)	22.696(2)	24.587(4)
α, deg	90	90	102.13(2)	90	97.68(2)
β, deg	95.16(2)	90	93.16(2)	91.21(2)	101.63(2)
γ, deg	90	90	99.35(2)	90	91.66(2)
V, Å^3	4553(2)	4947(3)	5733(2)	6769(2)	7239(2)
Z	4	4	4	4	4
density, g/cm^3	1.323	1.378	1.230	1.356	1.125
radiation	Mo Kα (λ = 71073 Å)	Mo Kα (λ = 71073 Å)	Mo Kα (λ = 71073 Å)	Mo Kα (λ = 71073 Å)	Mo Kα (λ = 71073 Å)
μ, mm^{-1}	0.102	0.259	0.881	0.784	0.766
abs corr	integration (X-Shape)	integration (X-Shape)	integration (X-Shape)	integration (X-Shape)	integration (X-Shape)
no. of reflns collected	19 302	61 574	38 787	44 805	52 224
no. of unique reflns	5797 [*R*(int) = 0.1715]	5405 [*R*(int) = 0.1594]	19 517 [*R*(int) = 0.0620]	11 915 [*R*(int) = 0.0496]	26 555 [*R*(int) = 0.1682]
no. of obsd refln	1578	4449	12 322	8213	5322
no. of data; params	5797, 615	5405; 353	19 517; 1334	11 915; 840	26 555; 1457
R_1[a], wR_2[b]	0.0591, 0.0822	0.1134, 0.2277	0.0390, 0.0762	0.0433, 0.1039	0.0941, 0.2233

[a] $R_1 = \sum||F_o| - |F_c||/\sum|F_o|$. [b] $wR_2 = \{\sum[w(F_o^2 - F_c^2)^2]/\sum[w(F_o^2)^2]\}^{1/2}$.

Mp: > 300 °C. IR (KBr, cm^{-1}): $\tilde{\nu}$ 3424 (ν(NH)) (w), 3064 (w), 2956 (m), 2906 (m), 2867 (w), 1640 (vs), 1612 (m), 1595 (m), 1552 (vs), 1516 (vs), 1499 (vs), 1453 (s), 1436 (s), 1390 (s), 1362 (w), 1311 (s), 1263 (vs), 1230 (s), 1183 (m), 1140 (m), 1096 (m), 1066 (w), 997 (w), 962 (m), 851 (s). ^{1}H NMR ($CDCl_3$, 300 MHz, 25 °C): δ 1.36 (s, 18 H, C(C*H*$_3$)$_3$), 1.76 (s, 6 H, C(C*H*$_3$)$_2$), 6.53 (m, 4 H, C*H*$^{(5A)}$), 6.72 (m, 4 H, C*H*$^{(3A)}$), 6.93 (m, 4 H, C*H*$^{(6A)}$), 7.11 (d, ^4J(H,H) = 2.4 Hz, 2 H, C*H*$^{(3/6)}$), 7.39 (d, ^4J(H,H) = 2.4 Hz, 2 H, C*H*$^{(1/8)}$), 7.97 (s, 2 H, C*H*N), 7.98 (s, 2 H, C*H*N), 12.66 (*ps*-t, *J* = 4.7 Hz, 2 H, N*H*). ^{13}C{^{1}H} NMR ($CDCl_3$ 75 MHz, 25 °C): δ 31.5 (C(*C*H$_3$)$_3$, 33.5 (C(*C*H$_3$)$_2$), 34.5 (C_q), 34.8 (C_q), 104.4 (m, *C*H$^{(3A)}$), 106.8 (C_q), 110.9 (d, ^2J(C,F) = 22.6 Hz, *C*H$^{(5A)}$), 116.9 (d, ^3J(C,F) = 9.1 Hz, *C*H$^{(6A)}$), 121.8 (*C*H$^{(3/6)}$), 125.2 (*C*H$^{(1/8)}$), 126.7 (C_q), 129.2 (C_q), 130.1 (m, *C*$^{(1A)}$), 144.9 (C_q), 145.6 (C_q), 149.4 (*C*HN), 153.7, 153.8 (dd, ^3J(C,F) = 11.5 Hz, ^1J(C,F) = 254.2 Hz C$^{(2A)}$C$^{(1A)}$-NH, ^3J(C,F) = 11.5 Hz, ^1J(C,F) = 250.1 Hz, C$^{(2A)}$C$^{(1A)}$=N), 148.6 (d(ps)-t, ^3J(C,F) = 4.53 Hz, ^1J(C,F) = 250.1 Hz, C$^{(4A)}$). ^{19}F NMR ($CDCl_3$, 282 MHz, 25 °C): δ −121.94 (s, br, *F*^{2}), −115.02 (m, *F*^{4}). EI-MS: *m*/*z* (%) 906.3 (27) [M$^+$], 793.3 (13) [M$^+$ − $C_6H_3F_2$], 767.3 (23) [M$^+$ − $C_7H_3NF_2$], 614.3 (22), 599.3 (21), 307.2 (18), 140.0 (19), 129.0 (100), 101.0 (26), 82.0 (20), 57.1 (43), 41.0 (26). EI-HRMS: *m*/*z* calcd for $C_{53}H_{46}F_8N_4O$, 906.3543; found, 906.3543. Anal. Calcd for $C_{53}H_{46}F_8N_4O$ (906.94): C, 69.93; H, 5.56; N, 5.72. Found: C, 69.72; H, 5.85; N, 5.51.

[^{Me2C6H3}Xanthdim](ZnEt)$_2$, 4. [^{Me2C6H3}Xanthdim]H_2 (300 mg, 0.342 mmol) was dissolved in tetrahydrofuran, and diethyl zinc (450 mg, 3.64 mmol) was added. After stirring the resulting bright honey-colored solution overnight all volatiles were removed under vacuum and the remaining yellow oil was dissolved in a small amount of diethyl ether. The product precipitated, and after removing all volatile compounds under vacuum again pure **4** was obtained in quantitative yield. Crystals suitable for X-ray analysis could be grown by storing a suspension of **4** in diethyl ether for 3 weeks.

IR (KBr, cm^{-1}): $\tilde{\nu}$ 2962 (m), 2855 (m), 1599 (s), 1576 (s), 1557 (m), 1460 (vs), 1440 (vs), 1382 (s), 1365 (s), 1309 (vs), 1261 (vs), 1245 (vs), 1224 (s), 1184 (s), 1162 (s), 1124 (s), 1092 (s), 1057 (s), 1016 (s), 987 (s), 955 (m), 877 (w), 857 (m), 797 (s), 781 (vs), 746 (m), 726 (m), 685 (m), 668 (w), 651 (w), 609 (w), 559 (w), 504 (w), 493 (w). ^{1}H NMR (thf-d_8, 300 MHz, 25 °C): δ 0.03 (q, ^3J(H,H) = 8.1 Hz, 4 H, C*H*$_2$), 0.846 (t, ^3J(H,H) = 8.1 Hz, 6 H, C*H*$_3$), 1.32 (s, 18 H, C(C*H*$_3$)$_3$), 1.67 (s, 6 H, C(C*H*$_3$)$_2$), 2.11 (ps-d, 12 H, C*H*$_3$), 6.74−6.84 (m, 12 H, C*H*$_{(N-aryl)}$), 7.04 (d, ^4J(H,H) = 2.4 Hz, 2 H, CH$^{(3/6)}$), 7.34 (d, ^4J(H,H) = 2.4 Hz, 2 H, CH$^{(1/8)}$), 7.75 (s, 4 H, C*H*N). ^{13}C{^{1}H} NMR (thf-d_8, 75 MHz, 25 °C): δ 0.0 (*C*H$_{2(ethyl)}$), 12.4 (*C*H$_{3(ethyl)}$), 15.2 (*C*H$_{3(N-aryl)}$), 20.4 (*C*H$_{3(N-aryl)}$), 31.6 (C(*C*H$_3$)$_3$), 33.2 (C(*C*H$_3$)$_2$), 34.6 (C_q), 35.4 (C_q), 104.1 (C_q), 121.2 (*C*H$^{(1/8)}$), 121.9 (*C*H$_{(N-aryl)}$), 126.3 (*C*H$_{(N-aryl)}$), 126.5 (*C*H$_{(N-aryl)}$), 127.8 (*C*H$^{(3/6)}$), 129.5 (C_q), 130.4 (C_q), 130.4 (C_q), 137.9 (C_q), 145.0 (C_q), 146.7 (C_q), 152.9 (C_q), 161.9 (*C*HN). Anal. Calcd for $C_{65}H_{78}N_4OZn_2$: C, 73.69; H, 7.42; N, 5.29 Found: C, 73.73; H, 7.48; N, 5.23.

[^{F2C6H3}Xanthdim](ZnEt(thf))$_2$, 5. 5 could be synthesized via the same procedure as described for **4** but employing [^{F2C6H3}Xanthdim]-H_2 as the starting material with quantitative yield. In contrast to **4**, **5** is soluble in diethyl ether. Large crystals could be obtained by slow evaporation of a tetrahydrofuran solution of **5**.

IR (KBr, cm^{-1}): $\tilde{\nu}$ 3067 (w), 2962 (m), 2901 (w), 2867 (w), 1612 (m), 1598 (s), 1503 (s), 1474 (vs), 1447 (s), 1429 (m), 1376 (m), 1327 (s), 1261 (s), 1196 (m), 1140 (m), 1099 (m), 967 (m), 847 (m), 810 (m). ^{1}H NMR (thf-d_8, 400 MHz, 25 °C): δ 0.11 (q, ^3J(H,H) = 8.0 Hz, 4 H, C*H*$_{2(ethyl)}$), 1.04 (t, ^3J(H,H) = 8.0 Hz, 6 H, C*H*$_{3(ethyl)}$), 1.31 (s, 18 H, C(C*H*$_3$)$_3$), 1.69 (s, 6 H, C(C*H*$_3$)$_2$), 6.69 (m, 4 H, C*H*$^{(5A)}$), 6.92 (m, 4 H, C*H*$^{(3A)}$), 7.01 (d, ^4J(H,H) = 2.4 Hz, 2 H, CH$^{(3/6)}$), 7.05 (m, 4 H, C*H*$^{(6A)}$), 7.35 (d, ^4J(H,H) = 2.4 Hz, CH$^{(1/8)}$), 7.9 (*ps*-d, *J*(H,H) = 2.0 Hz, 4 H, C*H*N). ^{13}C NMR (thf-d_8, 75 MHz, 25 °C): δ −1.39 (t, ^5J(C,F) = 5.0 Hz, *C*H$_{2(ethyl)}$), 13.0 (*C*H$_{3(ethyl)}$), 31.5 (C(*C*H$_3$)$_3$), 33.8 (C(*C*H)$_3$)$_2$), 34.7 (C_q), 35.2 (C_q), 104.7 (*ps*-t, ^2J(C,F) = 25.8 Hz, *C*H$^{(3A)}$), 104.9 (C_q), 111.9 (dd, ^2J(C,F) = 22.4 Hz, ^4J(C,F) = 3.7 Hz, *C*H$^{(5A)}$), 121.5 (*C*H$^{(3/6)}$), 126.3 (dd, ^2J(C,F) = 9.8 Hz, ^2J(C,F) = 3.0 Hz *C*H$^{(6A)}$), 127.0 (*C*H$^{(1/8)}$), 129.5 (C_q), 129.7 (C_q), 137.6 (dd, ^2J(C,F) = 9.7 Hz, ^4J(C,F) = 3.7 Hz, C$^{(1A)}$), 145.4 (br, 2 × C_q), 155.6 (dd, ^1J(C,F) = 246.2 Hz, ^3J(C,F) = 11.7 Hz, C$^{(2A)}$), 159.6 (dd, ^1J(C,F) = 246.2 Hz, ^3J(C,F) = 11.7 Hz, C$^{(4A)}$), 162.8 (*ps*-d, *C*HN). ^{19}F NMR (thf-d_8, 282 MHz, 25 °C): δ −123.42 (s, br, *F*^{2}), −117.30 (m, *F*^{4}). Anal. Calcd for $C_{65}H_{70}F_8N_4O_3Zn_2\cdot(C_4H_8O)_2$: C, 63.43; H, 6.27; N, 4.05. Found: C, 63.01; H, 6.37; N, 4.15.

[^{Me2C6H3}Xanthdim](Zn(SO$_2$Et))$_2$, 6. In a Young-Schlenk tube **4** (364 mg, 0.343 mmol) was dissolved in 5 mL of tetrahydrofuran. The tube was connected to a high-vacuum apparatus, cooled to −30 °C, and evacuated. An excess of dry SO_2 gas was condensed in portions to the solution, leading to a color change to red-orange. After stirring for 30 min at −30 °C the mixture was warmed to room temperature and all volatiles were removed under vacuum, yielding quantitatively a yellow solid with the stoichiometry [^{Me2C6H3}Xanthdim](Zn(SO$_2$Et))$_2$. Crystals suitable for X-ray analyses

could be obtained by slow evaporation of the solvent from a solution of **6** in a mixture of tetrahydrofuran (5 mL) and hexane (20 mL).

IR (KBr, cm^{-1}): $\tilde{\nu}$ 3063 (w), 2961 (s), 2911 (m), 2868 (w), 1602 (s), 1576 (m), 1481 (vs), 1463 (vs), 1442 (s), 1374 (m), 1321 (vs), 1254 (w), 1221 (m), 1072 (m), 989 (ν_{as}(SO)) (s), 963 (ν_s-(SO)) (s), 856 (w), 782 (m), 721 (w), 670 (w). ^{1}H NMR (C_6D_6, 300 MHz, 25 °C): δ 0.47 (m, 3 H, CH_3), 0.92 (s, br, 3 H, CH_3), 1.35 (s, 18 H, C(CH_3)$_3$), 1.65 (s, 6 H, C(CH_3)$_2$), 1.96−2.51 (m, br, 12 H, C$H_{3(N-aryl)}$, 4 H, C$H_{2(ethyl)}$), 6.72−7.11 (m, br, 8 H, C$H_{(N-aryl)}$), 7.38 (s, br, C$H^{(3/6,\ 1/8)}$), 7.45−7.72 (m, br, 4 H, C$H_{(N-aryl)}$), 7.91−8.10 (m, br, 4 H, CHN). ^{13}C NMR (C_6D_6, 75 MHz, 25 °C): δ 5.7 (br, CH$_{3(ethyl)}$), 15.3 (br, CH$_{(N-aryl)}$), 20.7 (br, CH$_{(N-aryl)}$), 31.5 (C(CH$_3$)$_3$), 34.2 (C(CH$_3$)$_2$), 34.9 (2 × C_q), 54.0 (br, CH$_{2(ethyl)}$), 101.6 (C_q), 121.0 (CH$^{(3/6)}$), 123.8 (CH$_{(N-aryl)}$), 123.9 (CH$_{(N-aryl)}$), 126.3 (CH$_{(N-aryl)}$), 128.1 (CH$^{(1/8)}$), 129.5 (C_q), 130.4 (C_q), 137.6 (br, C_q), 144.5 (C_q), 145.7 (br, C_q), 151.7 (br, C_q), 164.5 (br, CHN). MALDI-MS [$C_{65}H_{78}N_4O_5S_2Zn_2$] *m*/*z* (%): 1093 (83%), 1099.4 (100%), 1101.0 (76%), isotopic pattern for $M^+ - C_2H_5SO_2$. Anal. Calcd for $C_{65}H_{78}N_4O_5S_2Zn_2$: C, 65.59; H, 6.61; N, 4.71; S, 5.39. Found: C, 65.14; H, 6.84; N, 4.61; S, 5.27.

General Procedure for Copolymerization of Cyclohexene Oxide and CO_2 Using Catalysts 4, 5, and 6. The copolymerization reactions were performed in a Büchi tinyclave reactor. Cyclohexene oxide (3.92 g, 40 mmol) was added to the reactor in the glovebox under an inert atmosphere of argon. The catalyst (20 μmol, corresponding to 40 μmol of Zn) was placed on a glass boat in order to prevent premature mixing. Then the reactor was closed and transferred to a Schlenk line, where the atmosphere was exchanged for 8 atm CO_2. After saturation of the cyclohexene oxide with CO_2 was complete, the solution and the catalyst were mixed by tilting the reactor. The system was then heated to the desired temperature. The pressure of CO_2 was maintained at 8 atm. After the specified reaction time the heating was discontinued and the reactor was cooled in an ice bath to 5−10 °C, then the pressure was released and the reaction mixture was quenched by addition of CH_2Cl_2 and MeOH. All volatiles were evaporated *in vacuo* at 80 °C to obtain the polymer product as a crispy solid.

X-ray Diffraction Data Collection for [^{F2C6H3}Xanthdim]H_2, 4, 5, and 6. Single crystals of the compounds were selected in a cold stream of nitrogen. They were then mounted on top of a fiber and quickly frozen to −93 °C. Centered reflections were refined by least-squares calculations to indicate the unit cells. Unit cell and collection parameters for the complexes are listed in Table 6. Diffraction data were collected in the appropriate hemispheres and under the conditions specified also in Table 6. Two crystal structure determinations were performed for [^{F2C6H3}Xanthdim]H_2: the first one was performed for a crystal containing additional disordered chloroform solvent molecules that led to relatively high *R* values. In the second case the crystal did not include any solvent molecule, so that the *R* values are significantly lower. However, the resolution was higher in the former case (it thus forms the basis for the structure discussion), so that both results are listed in Table 6.

Solution and Refinement of the Structures of [^{F2C6H3}Xanthdim]-H_2, 4, 5, and 6. The structures were solved by direct methods (program: SHELXS-97)[13] and refined versus F^2 (program: SHELXL-97)[14] with anisotropic temperature factors for all non-hydrogen atoms. The final residuals are indicated in Table 6. The crystallographic data (apart from structure factors) of [^{F2C6H3}Xanthdim]-H_2, **4**, **5**, and **6** were deposited at the Cambridge Crystallographic Data Center as supplementary publication nos. CCDC 625190/637291, CCDC 625192, CCDC 625191, and CCDC 625193. Copies of the data can be ordered free of charge from the following address in Great Britain: CCDC, 12 Union Road, Cambridge CB2 1EZ (fax: (+44)1223-336-033; e-mail: deposit@ccdc.cam.ac.uk).

Acknowledgment. We are grateful to the Fonds der Chemischen Industrie, the BMBF, and the Dr. Otto Röhm Gedächtnisstiftung for financial support. K.C.H. is a DFG Emmy Noether fellow (2001−2007). We also would like to thank P. Neubauer for crystal structure analyses and Prof. J. Okuda and Dr. K. Beckerle (RWTH Aachen) for GPC measurements.

Supporting Information Available: This material is available free of charge via the Internet at http://pubs.acs.org.

OM070221E

(13) Sheldrick, G. M. *SHELXS-97*, Program for Crystal Structure Refinement; University of Göttingen, 1997.

(14) Sheldrick, G. M. *SHELXL-97*, Program for Crystal Structure Solution; University of Göttingen, 1997.